Polarized X-ray Absorption Spectroscopy of Cupric Chloride Dihydrate

Ingrid J. Pickering* and Graham N. George*

Stanford Synchrotron Radiation Laboratory, Stanford University, SLAC, P.O. Box 4349, MS 69, Stanford, California 94309-0210

Received November 10, 1994[⊗]

We report a detailed polarized single-crystal X-ray absorption spectroscopic study of $CuCl_2 \cdot 2H_2O$, with measurements at both the copper K-edge and the chlorine K-edge. The angular dependence of both dipole-allowed and quadrupole-allowed transitions is determined in detail for the copper K-edge. The formally dipole-forbidden, quadrupole-allowed Cu K-edge 1s → 3d transition behaves as a pure quadrupole transition, with no significant dipole contribution. The 1s → 3d transition is found to have predominantly $3d_{x^2-y^2}$ character, as expected, but evidence is also given for vacancies in a lower lying d orbital, possibly $3d_{xz}$, arising from the presence of $d\pi-d\pi$ bonding with the chloride ligands. The chlorine K-edge data show a strongly polarized pre-edge resonance at ~2821 eV, which can be interpreted in terms of a transition from the chlorine 1s orbital to an antibonding orbital with significant contributions from both chlorine 3p and the half-filled copper $3d_{x^2-y^2}$ orbital.

Introduction

X-ray absorption spectra can be broadly divided into two regions: the X-ray absorption near-edge spectrum and the extended X-ray absorption fine structure (EXAFS). EXAFS comprises the structure in the region 50−1500 eV above an X-ray absorption edge; it is fairly readily interpreted and is widely used as a quantitative tool in structural analysis.[1] The X-ray absorption near-edge spectrum is the spectral structure near the absorption edge (within ~50 eV), and this, in contrast to the EXAFS, is often rather difficult to interpret. The structure in the edge region arises from promotion of core electrons to bound states, and X-ray absorption edge spectra are thus very sensitive to the local electronic environment of the absorber atom.[1,2] In many cases, analysis of edge spectra is based on studies of well-characterized model compounds, often including polarized measurements.[3] With appropriate analysis, edge spectra can give rise to important insights into the electronic structure of the absorbing atom and edge spectra have been successfully used in numerous studies of metalloproteins, catalysts, superconductors, and a range of other materials [*e.g.* see ref 1 and references therein].

The X-ray absorption edge spectra of divalent copper species are probably the most intensively investigated among the transition metal ions, and considerable data, including many single-crystal studies, are available in the literature.[4−12] Indeed, the object of our present study, $CuCl_2 \cdot 2H_2O$, was among the very earliest compounds investigated by X-ray absorption edge spectroscopy.[4,13] We report herein a detailed investigation of the polarized edge spectra of $CuCl_2 \cdot 2H_2O$, at both the copper and the chlorine X-ray absorption K-edges.

Experimental Section

Sample Preparation. $CuCl_2 \cdot 2H_2O$ was obtained from Aldrich Chemical Co. and was used without further purification. Polarized X-ray absorption spectroscopy (XAS) measurements were carried out upon a single crystal of $CuCl_2 \cdot 2H_2O$ carefully cleaved along the $(\bar{1}01)$ cleavage plane to yield a crystal 0.23 × 0.70 × 3.50 mm, with the long dimension corresponding to the crystallographic *b* axis[14] and the largest face being $(\bar{1}01)$. The crystal was conveniently oriented by examination in a microscope with reference to its well-defined cleavage planes.[14] Polarized Cu K-edge XAS data sets were collected in our experiments by rotating the crystal around two distinct axes. The first rotation has an axis along [010] (the crystallographic *b* axis), which is oriented vertically, *i.e.* orthogonal both to the X-ray electric vector **e** and to the X-ray forward propagation vector **k**. Hence, both **e** and **k** precess in the (010) plane (the *a*−*c* plane) and are orthogonal to the $(\bar{1}01)$ face of the crystal. The angle α describes the angle between **e** and [100] (the *a* axis). In the second rotation, the **e** vector rotates between [010] (the *b* axis) and [101] (bisecting *a* and *c* at an angle 42.5° to *a*) in the $(\bar{1}01)$ face and the rotation is around the $(\bar{1}01)$ normal, which is also parallel to **k**. The angle β specifies the angle between **e** and [010] (the *b* axis) in the $(\bar{1}01)$ plane.

Data Collection. X-ray absorption spectroscopic measurements at the copper K-absorption edge were carried out on beamline X10C at the National Synchrotron Light Source,[15] and measurements at the

* To whom correspondence should be addressed.

[⊗] Abstract published in *Advance ACS Abstracts,* May 15, 1995.

(1) Koningsberger, D. C.; Prins, R. *X-ray Absorption Principles, Applications, Techniques of EXAFS, SEXAFS and XANES*; John Wiley and Sons: New York, 1988.
(2) Stöhr, J. *NEXAFS Spectroscopy*; Springer Verlag: Berlin, 1992.
(3) Brouder, C. *J. Phys.: Condens. Matter* **1990**, *2*, 701−738.
(4) Beaman, W. W.; Beaman, J. A. *Phys. Rev.* **1942**, *61*, 455−458.
(5) (a) Cotton, F. A.; Ballhausen, C. J.; *J. Chem. Phys.* **1956**, *25*, 617−619. (b) Cotton, F. A.; Hanson, J. P. *J. Chem. Phys.* **1956**, *25*, 619−623. (c) Chan, S. I.; Hu, V. W.; Gamble, R. C. *J. Mol. Struct.* **1978**, *45*, 239−266.
(6) Bair, R. A.; Goddard, W. A., III. *Phys. Rev.* **1980**, *B22*, 2767−2776.
(7) Kosugi, N.; Yokoyama, T.; Asakura, K.; Kuroda, H. *Chem. Phys.* **1984**, *91*, 249−256.
(8) Smith, T. A.; Penner-Hahn, J. E.; Berding, M. A.; Doniach, S.; Hodgson, K. O. *J. Am. Chem. Soc.* **1985**, *107*, 5945−5955.
(9) Hahn, J. E.; Scott, R. A.; Hodgson, K. O.; Doniach, S.; Desjardins, S. R.; Solomon, E. I. *Chem. Phys. Lett.* **1982**, *88*, 595−598.
(10) Yokoyama, T.; Kosugi, N.; Kuroda, H. *Chem. Phys.* **1986**, *103*, 101−109.
(11) Sano, M.; Komorita, S.; Yamatera, H. *Inorg. Chem.* **1992**, *31*, 459−463.
(12) Shadle, S. E.; Penner-Hahn, J. E.; Schugar, H. J.; Hedman, B.; Hodgson, K. O.; Solomon, E. I. *J. Am. Chem. Soc.* **1993**, *115*, 767−776.
(13) We note in passing that $CuCl_2 \cdot 2H_2O$ is a historic compound in another sense, in that at about the same time as the first XAS experiments[4] this compound was the subject of the first electron paramagnetic resonance spectroscopy experiments (Zavoisky, E. *J. Phys. USSR (Engl. Transl.)* **1942**, *9*, 245).
(14) (a) Engberg, A. *Acta Chem. Scand.* **1970**, *24*, 3510−3526. (b) Peterson, S. W.; Levy, H. A. *J. Chem. Phys.* **1957**, *26*, 220−221.
(15) Sansone, M.; Via, G. H.; George, G. N.; Meitzner, G.; Hewitt, R.; Marsch, J. In *X-ray Absorption Fine Structure*; Hasnain, S. S., Ed.; Ellis Horwood: New York, 1991; pp 656−658.

0020-1669/95/1334-3142$09.00/0

chlorine K-edge were carried out on beamline 6-2 at the Stanford Synchrotron Radiation Laboratory.[16] On X10C a Si(220) double-crystal monochromator was used, with an upstream vertical aperture of 0.1 mm, the optical cutoff of the downstream focusing mirror set to 15 keV, and typical storage ring operating conditions of 110−190 mA at 2.5 GeV. On 6-2, a Si(111) double-crystal monochromator was used, with the 54-pole wiggler at a field of 0.5 T and with the SPEAR storage ring containing 55-90 mA at 3.0 GeV. The copper K-edge X-ray absorption spectrum of microcrystalline $CuCl_2 \cdot 2H_2O$ was measured using two nitrogen-filled ion chambers, while the absorption spectrum of a copper metal foil calibration standard was simultaneously recorded using a third ion chamber. For the single-crystal Cu K-edge measurements, X-ray absorption was measured both as the transmittance and by monitoring the Cu Kα X-ray fluorescence excitation spectrum using an array of 13 intrinsic germanium detectors.[17] The fluorescence data were corrected for the distortions due to thickness effects (sometimes called self-absorption) by using an algorithm[18] similar to that used by others.[19] For the Cl K-edge, X-ray absorption was measured both by monitoring the X-ray fluorescence with a N_2-filled Stern−Heald−Lytle ion chamber detector[20] and by monitoring the total electron yield.

Data Analysis. The data were analyzed using the EXAFSPAK[21] suite of programs running on Digital Equipment Corp. VAXstation 4000 graphics workstations. Copper K-edge spectra were calibrated with reference to the lowest energy inflection point in the spectrum of the copper metal standard, assumed to be 8980.3 eV. Chlorine K-edge spectra were calibrated with reference to the lowest energy peak in the sulfur K-edge spectrum of sodium thiosulfate, assumed to be 2472.0 eV.[22]

The EXAFS oscillations $\chi(k)$ were quantitatively analyzed by curve-fitting.[23] The angular dependence of the EXAFS amplitude is approximated by plane-wave theory using the factor $3\cos^2\theta$, where θ is the angle between the X-ray polarization **e**-vector and the absorber−backscatterer vector. The EXAFS total amplitude and phase-shift functions (both polarized and unpolarized) were calculated by using the program *feff* (version 6.01) of Rehr and co-workers[24,25] using coordinates derived from the crystal structure.[14]

The background-subtracted edge spectra were normalized to the amplitude of the EXAFS spline function at X-ray energies just above the absorption edge (chosen as 9020 and 2850 eV for copper and chlorine K-edge spectra, respectively). The edge spectra were fitted using the EXAFSPAK program EDG-FIT, which uses nonlinear least-squares optimization to fit the data to a sum of pseudo-Voigt peaks plus an edge step function.[26]

A total of 19 single-crystal polarized Cu K-edge spectra plus the spectrum of the polycrystalline sample were fitted in the range 8970−9020 eV. The fitting summed 10 different peaks with common peak positions and peak widths for all orientations, varying only the peak amplitudes for the individual orientations. The pseudo-Voigt mixing parameter[26] was refined in initial fits to be 0.837 and was held invariant at this value for all peaks and edge steps in the final fits. For all the spectra, the edge step had a half-width at half-maximum of 3.0 eV and its energy was fixed at 9010 eV, chosen to be higher than the energies previously calculated for bound-state transitions in this system.[10] A total of 10 peaks were found necessary to fit all the data; while some of these were well resolved, others were found to have considerable overlap with nearby peaks. The amplitudes of these overlapping peaks were found to be highly correlated in the curve-fitting, and it was not considered possible to accurately deconvolute them; therefore, we chose to sum their amplitudes for all further analyses. The integrated areas of the peaks were normalized to the height of the edge step function for each fit, which was found to vary by less than 3% overall. Additionally the 1s → 3d peaks of the copper K-edge for all orientations were fitted separately in the range 8970−8984 eV so as to obtain a more accurate background. The 1s → 3d feature was fitted to a sum of two Gaussian peaks (a pseudo-Voigt mixing parameter of 1.0[26]), with a half-width at half-maximum of 1.02 eV and energies of 8978.62 and 8977.61 eV.

The chlorine K-edge data were fitted in the range 2810−2880 eV using six peaks for the four data sets (three polarized, plus the powder spectrum). In this case the pseudo-Voigt mixing parameter[26] was held constant at 0.55 for the pre-edge peaks and at 0.9 for the other peaks, and peak energies, widths, and amplitudes were allowed to vary, with the widths of the two pre-edge peaks at 2821.2 and 2822.6 eV constrained to be equal.

Detailed results for the deconvolutions of all spectra are given in the supplementary material.

Results and Analysis

The crystal structure of cupric chloride dihydrate has previously been determined using single-crystal X-ray and neutron diffraction.[14] $CuCl_2 \cdot 2H_2O$ crystallizes in the orthorhombic space group *Pmna*, with the unit cell parameters $a_0 = 8.04$, $b_0 = 3.72$, and $c_0 = 7.34$ Å.[14] It is composed of planar $CuCl_2(H_2O)_2$ molecules of point symmetry D_{2h}, with an additional very distant axial chlorine ligation[14] (see Figure 1). For the purposes of analysis of our data, we define a molecular axis system using the same convention as Yokoyama *et al.*,[10] with the *z* axis

(16) Bahr, C.; Chan, T.; Chin, J.; Elioff, T.; Halbach, K.; Harnett, G.; Hoyer, E.; Humphries, D.; Hunt, D.; Kim, K-J.; Lauritzen, T.; Lindle, D.; Shirley, D.; Tafelski, R.; Thompson, A.; Cramer, S.; Eisenberger, P.; Hewitt, R.; Stöhr, J.; Boyce, R.; Brown, G.; Golde, A.; Gould, R.; Hower, N.; Lindau, I.; Winick, H.; Yang, J.; Harris, J.; Scott, B. *Nucl. Instrum. Methods Phys. Res.* **1983**, *208*, 117−125.

(17) Cramer, S. P.; Tench, O.; Yocum, M.; George, G. N. *Nucl. Instrum. Methods Phys. Res.* **1988**, *A266*, 586−591.

(18) X-ray fluorescence thickness (self-absorption) corrections were calculated by numerical solution of the fluorescence equation (see ref 19b and references therein) for the crystal of size 0.23 × 0.70 × 3.50 mm, assuming a Cu Kα energy of 8048 eV.

(19) (a) Waldo, G. S.; Carlson, R. M. K.; Moldowan, J. M.; Peters, K. E.; Penner-Hahn, J. E. *Geochim. Cosmochim. Acta* **1991**, *55*, 801−814. (b) Troger, L.; Arvanitis, D.; Barberschke, K.; Michaelis, H.; Grimm, U.; Zschech, E. *Phys. Rev. B* **1992**, *46*, 3283−3289.

(20) (a) Stern, E.; Heald, S. *Rev. Sci. Instrum.* **1979**, *50*, 1579−1581. (b) Lytle, F. W.; Greegor, R. B.; Sandstrom, D. R.; Marques, E. C.; Wong, J.; Spiro, C. L.; Huffman, G. P.; Huggins, F. E. *Nucl. Instrum. Methods Phys. Res.* **1984**, *226*, 542−548.

(21) The EXAFSPAK program suite was developed by G.N.G. and is available by application in writing to the authors.

(22) Note that this value is slightly different from that used in our previous work on sulfur K-edges (George, G. N.; Gorbaty, M. L. *J. Am. Chem. Soc.* **1991**, *111*, 3182−3186). In the present study, we choose to use the calibration value of Hedman and co-workers (Hedman, B.; Frank, P.; Penner-Hahn, J. E.; Roe, A. L.; Hodgson, K. O.; Karlson, R. M. K.; Brown, G.; Cerino, J.; Hettel, R.; Troxel, T.; Winick, H.; Yang, J. *Nucl. Instrum. Methods Phys. Res.* **1986**, *A246*, 797−800) so that chlorine K-edge transition energies given in the present work can be directly compared with values in the literature cited below.

(23) The EXAFS oscillations $\chi(k)$ are given by the approximate equation

$$\chi(k) \simeq \sum_{i=1}^{n} \frac{N_i A_i(k,R_i)}{kR_i^2} e^{-2R_i/\lambda(k,R_i)} e^{-2\sigma_i^2 k^2} \sin\left[2kR_i + \alpha(k,R_i)\right]$$

where $A_i(k)$ and $\alpha_i(k)$ are the EXAFS total amplitude and phase-shift functions, respectively, k is the photoelectron wave number, N_i is the number of i-type atoms at a mean distance R_i from the absorber atom, λ_i is the photoelectron mean free path, and σ_i is the Debye−Waller factor, equal to the root-mean-square deviation of R_i. The summation is over all sets of inequivalent interactions. Polarized phase and amplitude interactions were calculated by defining the **e**-vector to lie along the *a*, *b*, and *c* axes using the capabilities built into *feff* 6.01.[24,25]

(24) Rehr, J. J.; Mustre de Leon, J.; Zabinsky, S. I.; Albers, R. C. *J. Am. Chem. Soc.* **1991**, *113*, 5135−5140.

(25) Mustre de Leon, J.; Rehr, J. J.; Zabinsky, S. I.; Albers, R. C. *Phys. Rev.* **1991**, *B44*, 4146−4156.

(26) The program EDG-FIT was used to perform least-squares fitting of the spectra to a sum of pseudo-Voigt peaks plus an edge step function. The anticipated spectral peak shape is a convolution of an (approximately) Gaussian and Lorentzian function, the former component resulting from monochromator broadening and the latter from core-hole lifetimes. In practice, this peak shape is well approximated by the pseudo-Voigt peak-shape function which is a simple sum of Lorenztian and Gaussian components, with a variable mixing (0 for pure Lorentzian and 1 for pure Gaussian). The edge-step function in EDG-FIT is approximated by the integral of a pseudo-Voigt function. The integrated intensity I of a peak of amplitude A, half-width Γ, and mixing m (where A, Γ, and m are determined by EDG-FIT) is given by $I = A\Gamma\{m(\pi/\ln 2)^{1/2} + (1 - m)\pi\}$.

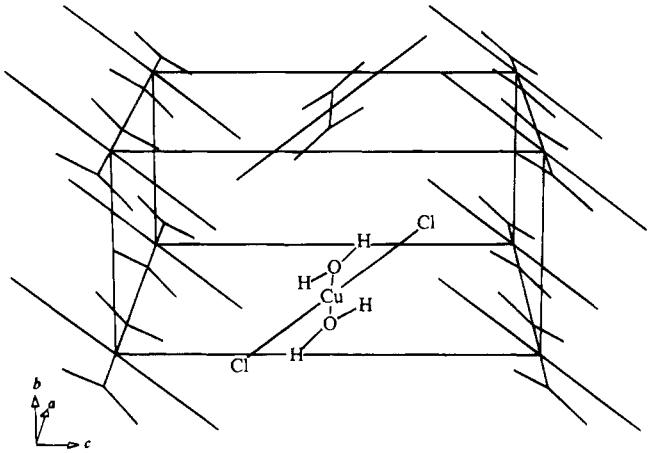

Figure 1. Crystal structure of $CuCl_2{\cdot}2H_2O$. The $CuCl_2(H_2O)_2$ molecules are planar with Cu−Cl and Cu−O distances of 2.28 and 1.94 Å, respectively. The axial Cu−Cl distance (not shown in the figure) is quite long at 2.94 Å, and the molecules can thus be considered essentially four-coordinate. The normals to the molecular planes of the two distinct orientations are at angles of ±38.7° to the crystallographic *b* axis and 90° to the *a* axis. The crystal has well-defined cleavage planes, parallel to (010), (101), and ($\bar{1}$01), which can be conveniently used to orient the sample.

normal to the $CuCl_2(H_2O)_2$ plane, the *x* axis parallel to the Cu−Cl bond, and the *y* axis parallel to the Cu−O bond.

Copper K-Edge EXAFS Spectra. Figure 2 shows the EXAFS Fourier transforms of $CuCl_2{\cdot}2H_2O$ with the X-ray polarization **e**-vector oriented along the crystallographic *a*, *b*, and *c* axes, together with the powder spectrum. The EXAFS spectra are readily interpreted in terms of the crystal structure. When the **e**-vector is oriented along the crystallographic *a* axis, **e** is oriented exactly along the Cu−O bonds and is normal to the Cu−Cl bonds (see Figure 1). The EXAFS should therefore be dominated by Cu−O EXAFS, with no significant contribution from Cu−Cl, and the amplitude of the observed Cu−O EXAFS should be about 3 times that of the powder spectrum. When the **e**-vector is oriented along the *b* and *c* axes, we expect no contribution from Cu−O and expect Cu−Cl EXAFS with an intensity about 1.2 and 1.8 times that of the powder, respectively. The EXAFS curve-fitting results are summarized in Table 1 and are in excellent agreement with the crystal structure.

It is interesting to note that we observe no significant contribution from distant 2.9 Å axial Cu−Cl interactions, even in the single-crystal measurements for orientations in which this interaction should be most intense. The result has bearing upon the copper K-edge EXAFS results of the protein plastocyanin.[27] While X-ray diffraction[28] indicates the presence of a 2.9 Å Cu−S(methionine) bond at the active site, polarized single-crystal EXAFS measurements at the copper K-edge failed to detect any such interaction.[27] Since chlorine and sulfur have very similar EXAFS scattering amplitudes, our results support the conclusion of Penner-Hahn *et al.*[27] that absence of detectable EXAFS is not unexpected for such long interactions due to large vibrational Debye−Waller factors[27] (in the protein, EXAFS cancellation due to other distant atoms is also possible).

Cu K-Edge Spectra. The 1s → 4p Transitions. The X-ray absorption cross section σ can be calculated from Fermi's "Golden rule", which can be expressed as

$$\sigma \propto \sum |\langle f|(\mathbf{e}\cdot\mathbf{p})e^{i(\mathbf{k}\cdot\mathbf{r})}|i\rangle|^2 \qquad (1)$$

where **e** is the X-ray electric vector, **p** is the electron momentum vector, **k** is the X-ray forward propagation vector, **r** is the transition operator (**x**, **y**, or **z**) in the molecular axis system, *f* and *i* are the final state and initial state wave functions, respectively, and the summation is over all initial states. In the dipole approximation, only the first term in the series expansion of the exponential is included, and $\sigma_D \propto \sum|\langle f|(\mathbf{e}\cdot\mathbf{p})|i\rangle|^2$. For a 1s orbital initial state (in the present case copper 1s) eq 1 reduces to $\sigma_D \propto |\sum_j e_j\langle f|r_j|i\rangle|^2$, where the coefficients e_j and r_j ($j = x, y, z$) are the direction cosines of the X-ray **e**-vector and transition operator, respectively (in the molecular axis system). The electric dipole-allowed transitions for K-edges are of the type 1s → *n*p ($\Delta l = \pm 1$, *l* being the azimuthal quantum number), and the most intense features in the edge spectrum are expected to correspond to such transitions.

As noted above, $CuCl_2{\cdot}2H_2O$ was among the very earliest compounds investigated by X-ray absorption edge spectroscopy.[4] In this early work, the state of the art did not extend to an assignment of the spectral features; nevertheless, it was recognized that the dipole-allowed 1s → 4p transitions should dominate the spectrum.[5] In general, tetragonal Cu(II) complexes show a shoulder or resolved peak about halfway up the Cu absorption K-edge, roughly midway between the 1s → 3d and the expected position of the 1s → 4p transitions. Because of its energy, this feature was at first assigned to a vibronically allowed 1s → 4s transition.[5] Later work by Bair and Goddard[6] used *ab initio* self-consistent-field configuration interaction (SCF−CI) calculations for a hypothetical molecular system, $CuCl_2$, to interpret this feature in $CuCl_2{\cdot}2H_2O$. These workers concluded that the shoulder structure was due to a group of transitions involving 1s → 4p transitions combined with a strong ligand-to-metal charge transfer, or shakedown transition.[29] Later work by Kosugi *et al.*,[7] also using SCF−CI calculations, supported this assignment for the related compound (creatininium)$_2CuCl_4$ and used single-crystal XAS data to show that the transition was highly polarized along the molecular *z* axis. At close to the same time, Smith *et al.*[8] reported a detailed single-crystal XAS study of a number of square planar Cu(II) complexes, including (creatininium)$_2CuCl_4$. These workers, however, preferred an assignment of a 1s → 4p_z transition, based on multiple scattered-wave Xα calculations, and for a while the assignment of this transition was controversial. At present, there is widespread agreement that the assignment of 1s → 4p + ligand-to-metal charge transfer shakedown is correct,[12] and the former controversy appears to be resolved.

Yokoyama *et al.*[10] reported a polarized copper K-edge study of a single crystal of cupric chloride dihydrate and used SCF−CI molecular orbital calculations to interpret the spectra. These workers reported spectra of two orientations: one with the X-ray polarization **e**-vector parallel to the crystallographic *b* axis and the other with **e** perpendicular to *b* in the (101) crystal cleavage plane. Unfortunately, Yokoyama *et al.* misinterpreted the crystallography in that they assumed that the planar $CuCl_2(H_2O)_2$ molecules were aligned with their normals along the crystal-

(27) Penner-Hahn, J. E.; Murata, M.; Hodgson, K. O.; Freeman, H. C. *Inorg. Chem.* **1989**, *28*, 1826−1832.

(28) Colman, P. M.; Freeman, H. C.; Guss, J. M.; Murata, M.; Norris, V. A.; Ramshaw, J. A. M.; Venkaptappa, M. P. *Nature* **1978**, *272*, 319−324.

(29) The 1s → 4p + ligand-to-metal charge transfer resonance can be rationalized as follows. When the metal 1s electron is ejected by X-ray absorption, the resulting core hole (which can be viewed as an increased nuclear charge) causes the metal 3d levels to relax to deeper binding energies. As a result of this, a ligand p to metal $3d_{x^2-y^2}$ transition (previously "uphill", now "downhill") occurs concomitantly with excitation of the 1s electron to the 4p level, *i.e.* $[1s^2\ 4p^0][3d^9\ L^2]$ → $[1s^1\ 4p^1][3d^{10}\ L^1]$. Thus, this shakedown resonance (a two-electron event) is shifted to lower energy relative to the pure 1s → 4p transition by the ligand-to-metal charge transfer energy.

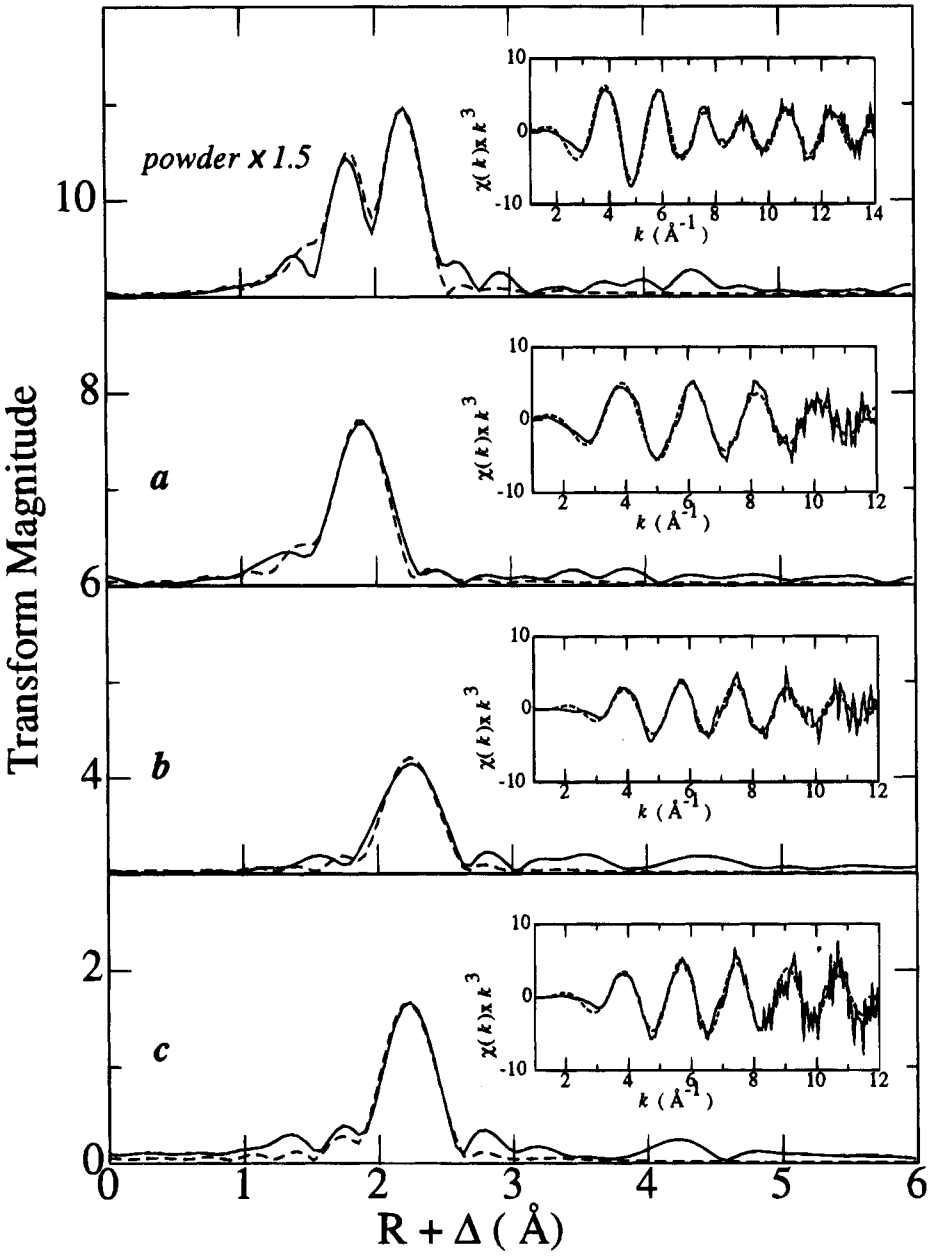

Figure 2. Polarized single-crystal and powder Cu K-edge EXAFS spectra of $CuCl_2 \cdot 2H_2O$. In the main figure, the solid lines show the Fourier transforms of the EXAFS data and the dashed lines the Fourier transforms of the fit from the curve-fitting analysis, the numerical results of which are given in Table 1. The corresponding plots of the raw and fitted k^3-weighted EXAFS data are shown in the insets.

Table 1. EXAFS Curve-Fitting Results for Powder and Single-Crystal Cu K-Edge EXAFS Spectra of $CuCl_2 \cdot 2H_2O$[a]

	Cu−Cl			Cu−O		
	N	R (Å)	σ^2 (Å^2)	N	R (Å)	σ^2 (Å^2)
polycrystalline	2.0	2.264(8), *2.275*	0.0051(4)	2.0	1.918(16), *1.925*	0.0051(10)
a axis [100]				1.8(3)	1.951(11)	0.0051
b axis [010]	2.1(3)	2.297(15)	0.0051			
c axis [001]	1.7(4)	2.288(15)	0.0051			

[a] The EXAFS Fourier transforms and EXAFS spectra are shown in Figure 2. The k-ranges used were 1−14 Å^{-1} for the powder and 1−12 Å^{-1} for the single-crystal data. Because of the high correlation between N and σ^2 in the curve-fitting, the single-crystal σ^2 values were held constant at the powder spectrum values during the fit. The values in parentheses are the estimated 95% confidence limits obtained from the diagonal elements of the covariance matrix of the least-squares fit. For the powder spectrum, the bond lengths in italics are those derived from neutron diffraction.[14] For the single-crystal data, scattering paths that had amplitudes lower than 5% of the largest were not included (*e.g.*, Cu−Cl was omitted for **e** along *a*).

lographic *b* axis.[10] Examination of the crystal structure[14] indicates that the $CuCl_2(H_2O)_2$ molecules are in fact arranged in a zigzag manner when viewed down [100], with the normal to the $CuCl_2(H_2O)_2$ plane at the not inconsiderable angle of 38.7° to the crystallographic *b* axis (see Figure 1).

Figures 3 and 4 show polarized single-crystal Cu K-edge X-ray absorption spectra. Figure 3 shows the Cu K-edge with the **e**-vector oriented along the crystallographic *a*, *b*, and *c* axes, compared with the powder spectrum, and the peak deconvolution fits for these orientations. Excluding the edge step function and the 1s → 3d transition at ~8979 eV, six distinct spectral features were found to be necessary for adequate analysis of

the data from all orientations (see Experimental Section for the methods used and supplementary material for full deconvolution results). It is important to note that these features, rather than being discrete transitions, may well be comprised of several transitions with similar energies (within the observed line width). These features are labeled A−F in Figure 3, in order of increasing energy. Figure 4A shows the angular variation of the absorption spectrum as the crystal orientation is varied so that the **e**-vector rotates from [100] to [001] in the (010) plane (from *a* through *c* in the *a*−*c* plane), and Figure 4B shows the variation when the crystal is rotated so that the **e**-vector rotates from [010] (the *b* axis) to [101] (close to the *a*−*c* bisector) in the (10$\bar{1}$) plane, *i.e.* with **e** remaining parallel to the crystal cleavage plane. The features A−F are identified in Figure 4, and Figure 5 shows polar plots of the angular variation in intensity of A−F. It is apparent from these figures that many of the major features of the spectrum show a marked anisotropy. In addition to the dipole transitions, the 1s → 3d transition also shows significant anisotropy and as this is of particular interest it will be discussed in detail in the next section.

The angular variation of the intensity I of the dipole-allowed transitions A−F can be described in terms of the intensities I_x, I_y, and I_z, along the molecular x, y, and z axes, respectively. As discussed above, the crystal structure[14] (Figure 1) indicates that the molecular z axes of the two distinct molecules in the unit cell are inclined at an angle ϵ to the crystallographic b axis (2ϵ to each other) where $\epsilon = 38.7°$. It can readily be shown that, for $CuCl_2{\cdot}2H_2O$, the angular variation in transition intensity I is given by eq 2, where e_a, e_b, and e_c are the direction cosines

$$I = I_y e_a^2 + (I_x \sin^2\epsilon + I_z \cos^2\epsilon) e_b^2 + (I_x \cos^2\epsilon + I_z \sin^2\epsilon) e_c^2 \quad (2)$$

of the X-ray **e**-vector with respect to the crystallographic axis system (*a*, *b*, *c*). The observed intensities for all of the orientations[30] were fitted to eq 2 to yield estimates of I_x, I_y, and I_z for each of the features A through F, and these results are summarized in Table 2. The solid lines in Figure 5 are calculated curves generated from eq 2 using the values given in Table 2. Excellent agreement is observed between the experimental and calculated curves. For the higher energy features (E, F, and possibly also D), the uncertainty in the position of the absorption-edge threshold means that the intensities of these features relative to those at lower energies may not be accurately estimated.

The data in Table 2 show that feature A, assigned as a group of 1s → 4p + ligand-to-metal charge transfer shakedown transitions, is most intense along the molecular z axis, although it also has significant intensity along both x and y. This is in quantitative agreement with the calculations of Yokoyama *et al.*,[10] who predict relative intensities for this transition of 0.09, 0.19, and 1.0 along the molecular x, y, and z axes, respectively, which compare well with our observed values of 0.13, 0.31, and 1.0 (Table 2). The other spectral features which are resolved by our curve-fitting analysis of the edge spectra show similar quantitative agreement with calculated intensities and positions,[10] and on this basis, we suggest possible assignments for these features in Table 2.

The Cu K-Edge 1s → 3d Transition. The smallest resolved feature in the spectrum is the small peak near 8980 eV, the formally dipole-forbidden 1s → 3d transition. Copper in $CuCl_2(H_2O)_2$ has a formally cupric oxidation state, with a $3d^9$ configuration and only a single vacancy in the 3d shell, and we expect the half-occupied ground state molecular orbital to have both copper $3d_{x^2-y^2}$ and ligand σ character. Some contribution from $3d_{z^2}$ is also expected in the ground-state wave function for the D_{2h} site symmetry of $CuCl_2(H_2O)_2$, but this will be small, being only about 7%.[31] In general, 1s → *n*d transitions gain intensity by virtue of being quadrupole allowed ($\Delta l = \pm 2$) and, in noncentrosymmetric complexes, by mixing of metal *n*p levels with the d levels, which confers some dipole-allowed character. In the case of $CuCl_2(H_2O)_2$, the site symmetry is centrosymmetric (D_{2h}) and we therefore expect rigorously no mixing of metal p orbitals with no dipole-allowed intensity from this mechanism. The electric quadrupole term for the absorption cross section σ_Q is given by the second term in the series expansion of the exponential in eq 1: $\sigma_Q \propto \sum|\langle f|(\mathbf{e}\cdot\mathbf{p})(\mathbf{k}\cdot\mathbf{r})|i\rangle|^2$. This shows that the intensity of quadrupole transitions will depend not only upon the orientation of the X-ray **e**-vector but also upon the orientation of the X-ray forward scattering vector **k**. Proceeding in a manner similar to that for the dipole-allowed 1s → *n*p transitions (above), we find that for 1s → *n*d transitions

$$\sigma_Q \propto \left|\sum_j \sum_n e_j k_n \langle f|r_j r_n|i\rangle\right|^2 \quad (3)$$

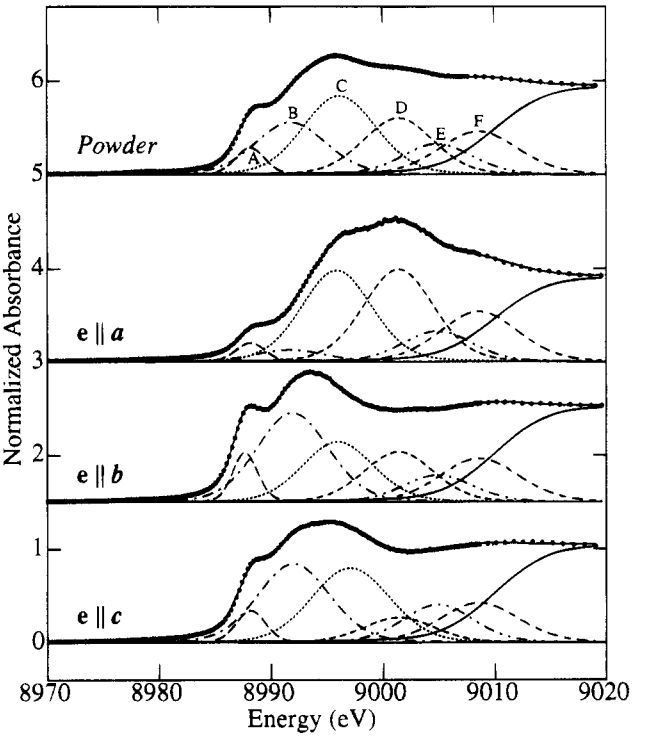

Figure 3. Edge deconvolution of the Cu K-edge spectra of polarized single-crystal and powder $CuCl_2{\cdot}2H_2O$. The experimental data points are shown as dots, with the total fitted curve as a solid line through the points. The edges were fitted to sums of a pseudo-Voigt step function (solid line) plus a total of nine pseudo-Voigt peaks (excluding the 1s → 3d transition; see below), having the same widths and energies for each of the orientations studied; numerical and graphical results of all the fits are given in the supplementary material. Features A−C are each a sum of two pseudo-Voigt peaks whereas features D−F are single peaks (see text). Polar plots of the variation in intensity of fetures A−F as a function of orientation are given in Figure 5.

(30) For the rotation of **e** and **k** in the (010) plane (Figure 4A, Figure 6), $\mathbf{e}_\alpha = (e_a, e_b, e_c) = (\cos\alpha, 0, \sin\alpha)$ and $k_\alpha = (-\sin\alpha, 0, \cos\alpha)$, where α is measured from [100]. For the rotation of **e** in the (10$\bar{1}$) plane (Figure 4B, Figure 7), $\mathbf{e}_\beta = (\cos\alpha_0 \sin\beta, \cos\beta, \sin\alpha_0 \sin\beta)$ and $\mathbf{k}_\beta = (-\sin\alpha_0, 0, \cos\alpha_0)$, where β is measured from [010] and $\alpha_0 = 42.5°$.

(31) Hitchman, M. A.; McDonald, R. G.; Riley, M. J. *Inorg. Chem.* **1984**, *23*, 2359−2361.

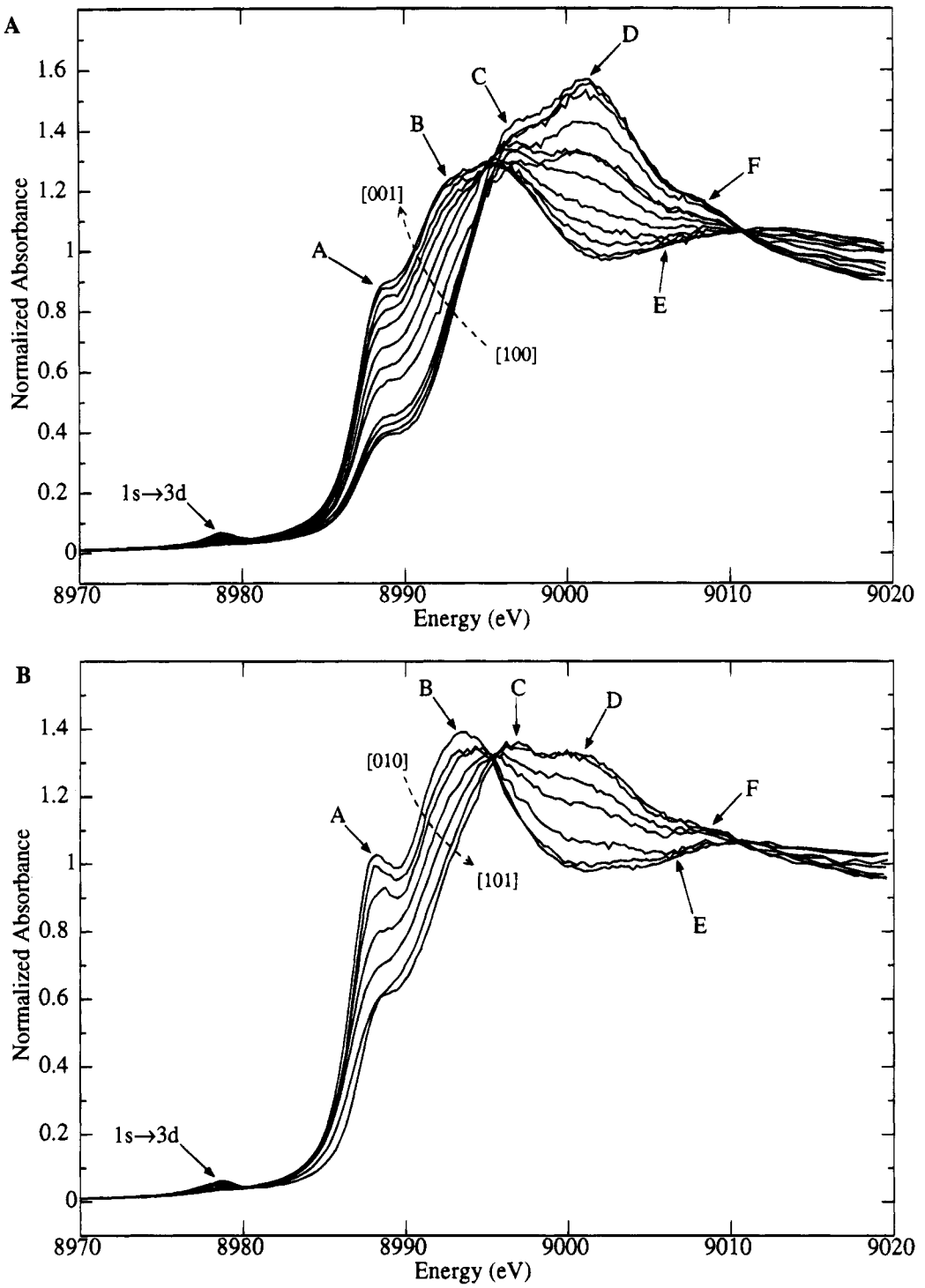

Figure 4. Cu K-edge spectra of $CuCl_2 \cdot 2H_2O$ as a function of orientation of the X-ray **e**-vector: (A) **e** rotated in the (010) plane, between [100] and [001]; (B) **e** rotated in the ($\bar{1}$01) plane between [010] and [101].

where the coefficients e_j and k_n ($j, n = x, y, z$) are the direction cosines of **e** and **k**, respectively, in the molecular axis system.[32]

The orientation dependence of the Cu K-absorption edge 1s → 3d transition of (creatininium)$_2CuCl_4$, which contains the planar $CuCl_4^{2-}$ unit (point group D_{2h} with only slight distortion from D_{4h}), has been measured in an elegant polarized single-crystal XAS study by Hahn *et al.*[9] The copper in this complex has the same site symmetry as $CuCl_2(H_2O)_2$, and both complexes contain square planar copper in a rigorously centrosymmetric coordination. Hahn *et al.*[9] observed a 90° periodicity in the intensity of the 1s → 3d transition, when **e** and **k** were rotated in the plane perpendicular to the crystallographic *c* axis, which is approximately in the molecular *x*−*y* plane for both the distinct molecular orientations in the unit cell, with the maximal intensity at approximately 45° to the molecular *x* axis. As pointed out by Hahn *et al.*,[9] such periodicity is expected for the predominantly copper $3d_{x^2-y^2}$ ground state orbital of the square planar Cu(II). These workers also observed an isotropic component of approximately 25% of the maximal intensity of the 1s → 3d

(32) Evaluation of the matrix elements $\langle f|r_j r_n|i\rangle$ using spherical harmonics describing atomic orbitals provides generalized approximate expressions for the angular dependence of polarized spectra for s → d quadrupole-allowed transitions to the five d orbitals: $\sigma_Q(d_{xy}) \propto (e_x k_y + e_y k_x)^2$, $\sigma_Q(d_{xz}) \propto (e_x k_z + e_z k_x)^2$, $\sigma_Q(d_{yz}) \propto (e_y k_z + e_z k_y)^2$, $\sigma_Q(d_{x^2-y^2}) \propto (e_x k_x - e_y k_y)^2$, and $\sigma_Q(d_{z^2}) \propto (2e_z k_z - e_x k_x - e_y k_y)^2$. A more complete treatment of the angular dependence of quadrupole-allowed transitions is given by Brouder.[3]

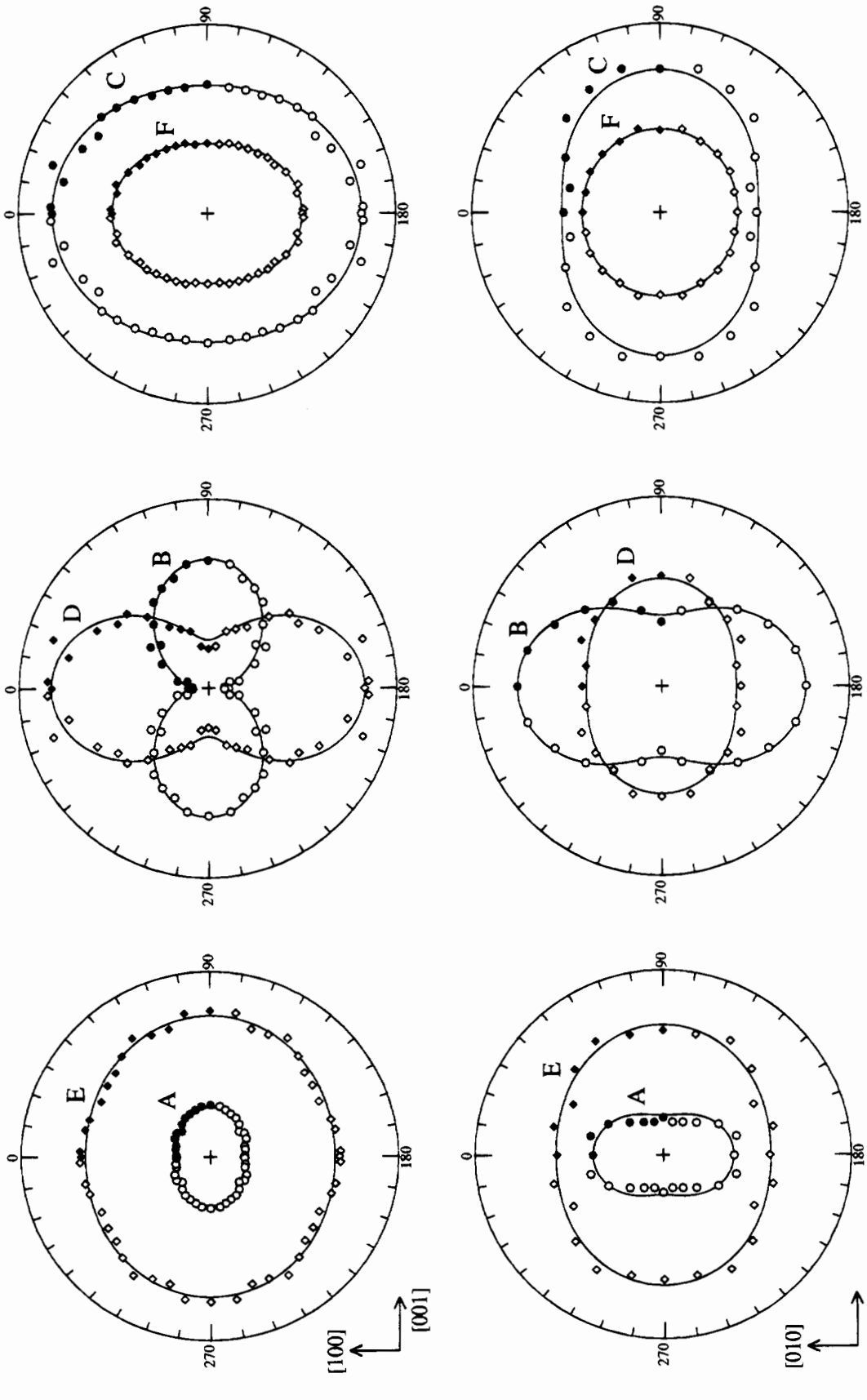

Figure 5. Cu K-edge dipole-allowed transition intensites as a function of e-vector orientation for $CuCl_2{\cdot}2H_2O$. The filled symbols are the relative intensities of the features A–F of Figures 3 and 4, obtained by edge deconvolution. The open symbols are duplicates of the filled ones generated by mirroring. The solid lines are calculated intensities generated using the results of a least-squares fitting procedure to obtain the components of the dipole intensity along the molecular axes (given in Table 2).

Table 2. Polarized Single-Crystal $CuCl_2 \cdot 2H_2O$ X-ray Copper K Absorption Edge Fitting Analysis[a]

feature	energy (eV)	I_x	I_y	I_z	possible assnt[b]
A[c]	8987.56,[d] 8988.17[e,f]	0.30			$1s \rightarrow 4p_x$ + LMCT
			0.68		$1s \rightarrow 4p_y$ + LMCT
				2.21	$1s \rightarrow 4p_z$ + LMCT
B[c]	8991.54,[d] 8992.90[f]	5.19			$1s \rightarrow 5p_x$ + LMCT
			1.15		
				8.98	$1s \rightarrow 5p_z$ + LMCT, $1s \rightarrow 4p_z$ + CI
C[c]	8995.90,[e] 8998.50[f]	9.35			$1s \rightarrow 5p_x$
			8.03		$1s \rightarrow 5p_y$ + LMCT
				2.41	$1s \rightarrow 4p_z$
D	9001.40	0.00			
			8.13		$1s \rightarrow 5p_y$ + CI, $1s \rightarrow 5p_y$
				6.39	$1s \rightarrow 5p_z$
E	9004.90	4.34	2.60	0.89	
F	9008.61	2.77	4.92	4.88	

[a] Results of a least squares curve-fitting analysis of the data shown in Figure 5 from eq 2, using a specially written computer program to obtain values for dipole-allowed intensities I_x, I_y, and I_z along the molecular x, y, and z axes. [b] Possible assignments are suggested on the basis of the SCF–CI calculations of Yokoyama *et al.*[10] Only the strongest transitions are identified. [c] For the features A–C a subtle, but significant, anisotropy in the peak energy was observed. This anisotropy was accounted for in the program EDG-FIT by using two peaks of fixed width, fixed energy, and variable amplitude. Because the amplitudes of these features were very highly correlated in the curve-fitting, it was not possible to accurately deconvolute them, and their intensities have therefore been summed. [d] Maximal along the molecular z axis. [e] Maximal along the molecular y axis. [f] Maximal along the molecular x axis.

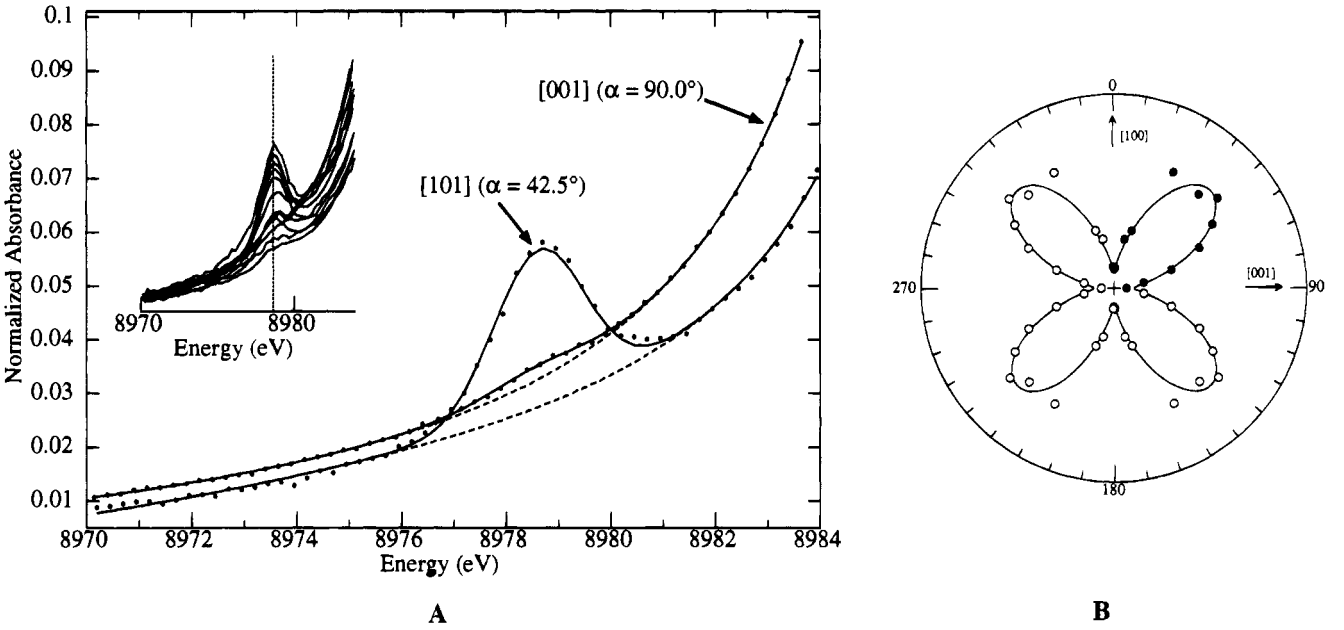

Figure 6. (A) Detail of the $1s \rightarrow 3d$ transition with both **e** and **k** rotating in the [010] plane. α is the angle between **e** and [100] in this plane. The points are the experimentally observed data, the solid lines the results of the deconvolution, and the dashed lines the background functions from the deconvolution. The inset shows the range of spectra obtained for this rotation. Note that the peak is invariant in both energy and width. (B) Variation in intensity of the $1s \rightarrow 3d$ transition as a function of angle α (0° corresponds to **e** along [100] and **k** along [001]). The filled symbols are the relative intensities extracted from fits such as shown in FIgure 6A, and the solid line is a least-squared fit of the intensity to the function $A \sin^2(2\alpha) + B$.

transition and attributed this to a combination of misalignment of the molecules in the unit cell, vibronically allowed dipole transitions, and imperfect polarization of the X-ray beam.[9,12]

Figure 6 shows the orientation dependence of the $CuCl_2 \cdot 2H_2O$ $1s \rightarrow 3d$ transition when the crystal is rotated so that the **e** and **k** rotate in the (010) plane (the crystallographic $a-c$ plane). The observed orientation dependence shows well-defined nodes, with a 90° repeat and a maximum intensity at 45° to [100] (Figure 6). The 90° repeat is characteristic of the dependency on both **e** and **k** of quadrupole transitions and occurs when both are rotated in the same plane. Our results are similar to those of Hahn *et al.*,[9] except that we observe the somewhat smaller intensity at $\alpha = 0$ and 90° of approximately 8% of maximal intensity (Figure 6A), rather than ~25% observed for $(creatininium)_2CuCl_4$ by Hahn *et al.*[9] The solid line in Figure 6B is the calculated curve for a $1s \rightarrow 3d_{x^2-y^2}$ transition,[33] from eq 3, accounting for the two distinct molecules in the crystallographic unit cell. The data appear entirely consistent with the assignment of the feature to an essentially pure quadrupole $1s \rightarrow 3d_{x^2-y^2}$ transition, with negligible intensity from other sources. The small (~8% of maximal, Figure 6) intensity at the nodes is low enough to be completely explained by incomplete polarization of the X-ray beam[34] and by possible slight inaccuracies in crystal alignment.

Figure 7 shows the orientation dependence of the $1s \rightarrow 3d$ transition when the crystal is rotated about the **k**-vector, so that

(33) For an $s \rightarrow d_{x^2-y^2}$ transition, the angular variation in X-ray absorption is approximately described by $\sigma_Q(d_{x^2-y^2}) \propto (e_x k_x - e_y k_y)^2$.[32] For the rotation of **e** and **k** in the (010) plane (Figure 6), this reduces to $\sigma_Q(d_{x^2-y^2}) \propto (\cos^2 \epsilon + 1)^2 \sin^2 2\alpha$. For the rotation of **e** about **k** in the (101) plane (Figure 7), $\sigma_Q(d_{x^2-y^2}) \propto (\cos^2 \alpha_0)[\sin^2 2\epsilon \cos^2 \beta + 4(\cos^2 \epsilon + 1)^2 \sin^2 \alpha_0 \sin^2 \beta]$.

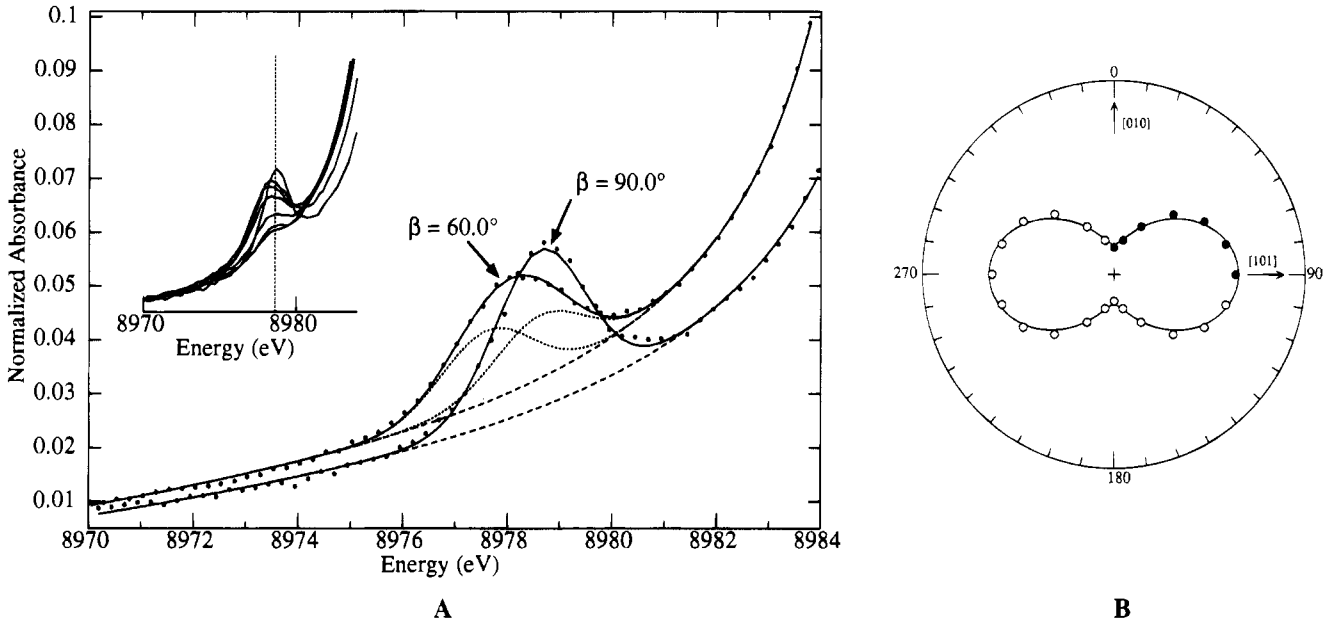

Figure 7. (A) Detail of the 1s → 3d transition for **e** rotating in the ($\bar{1}$01) plane and **k** along the (101) plane normal. β is the angle between **e** and [010] in this plane. The points are the experimentally observed data, the solid lines the results of the deconvolution, and the dashed lines the background functions from the deconvolution. The dotted lines show the deconvolution using two Gaussian peaks, the first at an energy of 8978.62 eV (that of the peak in Figure 6A) and the second at an energy of 8977.61 eV. The inset shows the range of spectra obtained for this rotation. Note the subtle but significant shift in both energy and width of the peak (compare with (Figure 6A), which is indicative of a contribution from a second, lower energy, resonance. (B) Variation in intensity of the 1s → 3d transition as a function of angle β. 0° corresponds to **e** along [010]. The filled symbols are the relative intensities extracted from fits such as shown in Figure 6A, and the solid line is a least-squared fit of the intensity to the function $A \sin^2 \epsilon + B$.

the **e**-vector rotates in the ($\bar{1}$01) plane. Interestingly, the 1s → 3d peak is observed both to shift to a lower energy and to significantly broaden as **e** moves away from the $a-c$ plane. We note in passing that this behavior would not have been observed if XAS data at only a small number of directions had been measured (typically with **e** along a, b, and c in previous studies), illustrating a major advantage of collecting a detailed series of orientations. This behavior of the 1s → 3d peak can be explained in terms of an additional 1s → 3d transition to an orbital having an energy approximately 1.0 eV lower than the $3d_{x^2-y^2}$ orbital (see the deconvolution in Figure 7A). A possible explanation for such 3d vacancies is the presence of $d\pi-d\pi$ bonding between copper and the chloride ligands, which seems likely from the weakly *trans*-directing properties of the ligand;[35] a Cl $3d_{xz}$–Cu $3d_{xz}$ π bond would produce holes in the formally filled Cu $3d_{xz}$ orbital which would be expected to lie about 1.0 eV lower in energy than the $3d_{x^2-y^2}$ orbital. From eq 3 and the crystal structure, we would expect a 1s → $3d_{xz}$ transition to have the same periodicity as 1s → $3d_{x^2-y^2}$ when **e** and **k** are rotated in the (101) plane (this is because the molecular $x-y$ plane is significantly inclined to the $a-c$ plane) (Figure 6) and a $A \sin^2 \beta + B$ dependence when the **e**-vector is rotated in the ($\bar{1}$01) plane (*i.e.* declining intensity as **e** is moved away from (101), (Figure 7). This predicted behavior is entirely consistent with our observations, although the resolution of the two 1s → 3d transitions was insufficient for us to accurately deconvolute the individual angular dependencies for each.

Hitchman and co-workers have examined the single-crystal polarized electronic and electron paramagnetic resonance spectra of $CuCl_2(H_2O)_2 \cdot 4(C_6H_5)PO$.[31,36] This compound contains one $CuCl_2(H_2O)_2$ molecule per unit cell and differs from $CuCl_2 \cdot 2H_2O$ in lacking the long axial 2.9 Å chlorine ligands.[37] According to the assignments of the electronic spectra given by McDonald and Hitchman,[36] and converting to our coordinate system, transitions from the $3d_{x^2-y^2}$ occur at 1.64, 1.88, 1.91, and 2.20 eV, to the $3d_{xy}$, $3d_{xz}$, $3d_{yz}$, and $3d_{z^2}$ orbitals, respectively. Our deconvolution of the 1s → 3d pre-edge feature indicates that the separation of the two 1s → 3d peaks must be less than ~1.5 eV; otherwise, a resolved doublet would be observed in the spectrum (not illustrated). We expect the separation of the 1s → $3d_{x^2-y^2}$ and the 1s → $3d_{xz}$ transitions to differ from the value of 1.88 eV obtained from the optical spectra[36] due to the presence of axial chloride ligands in $CuCl_2 \cdot 2H_2O$ not present in the compound investigated by Hitchman and co-workers[31,36] and due to the presence of a core-hole in the final state probed by XAS.[38] In addition, we expect differences in the interelectronic Coulomb and exchange energies between X-ray and optical transitions.[39] Following George *et al.*,[39] we estimate a difference between X-ray and optical splittings of approximately −0.23 eV arising from these effects,[40] and thus the X-ray assignment seems quite consistent with the optical splittings.

Similar $d\pi-d\pi$ bonding involving $3d_{xy}$ orbitals also provides a possible explanation for the anomalous intensity at the nodes of the 1s → $3d_{x^2-y^2}$ transition which was observed by Hahn *et*

(34) In independent measurements under conditions similar to those used for the copper K-edge study described herein, we estimate the polarization of the beam to be better than 90%. This estimate was made by monitoring the changes in X-ray scattering from a flat piece of kapton film when the plane of the film was inclined at 0 and 45° to **e** and fixed at 45° to **k**.

(35) See for example: Cotton, F. A.; Wilkinson, G. *Advanced Inorganic Chemistry*, 5th ed.; John Wiley and Sons: New York, 1988. Greenwood, N. N.; Earnshaw, A. *Chemistry of the Elements*; Pergamon Press: Oxford, U.K., 1984.

(36) McDonald, R. G.; Hitchman, M. A. *Inorg. Chem.* **1990**, *29*, 3074–3081.

(37) Dunaj-Jurco, M.; Kozisek, J.; Ancyskina, A.; Onderjovic, G.; Makanova, D.; Gazo, J. *J. Chem. Soc., Chem. Commun.* **1979**, 654–655.

(38) In the "effective $Z + 1$ approximation", the presence of a core hold (1s for a K-edge) causes the XAS data to more closely resemble optical splitting from the compound with $Z + 1$ (*i.e.* Zn, for a Cu edge in the present case.)

(39) George, G. N.; Cleland, W. E.; Enemark, J. H.; Smith, B. E.; Kipke, C. A.; Roberts, S. A.; Cramer, S. P. *J. Am. Chem. Soc.* **1990**, *112*, 2541–2548.

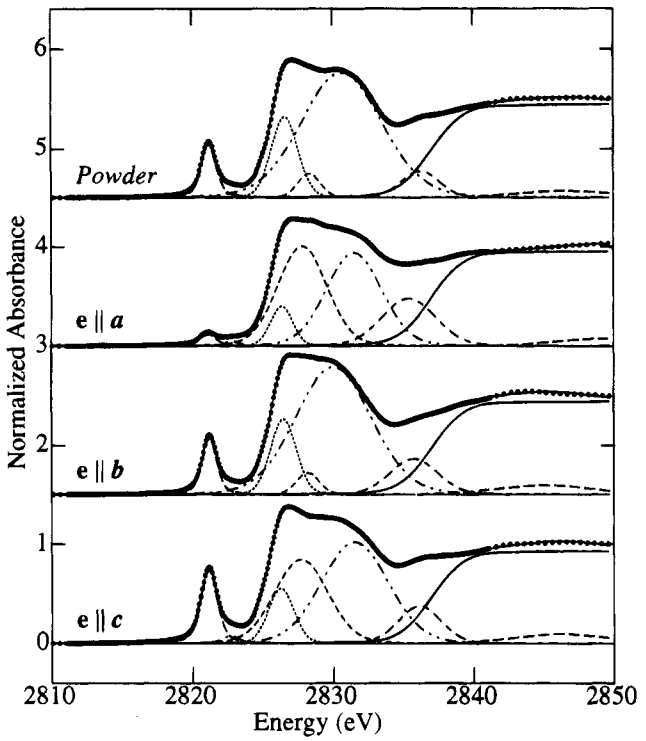

Figure 8. Edge deconvolution of the Cl K-edge spectra of polarized single-crystal and powder $CuCl_2 \cdot 2H_2O$. The experimental data points are shown as dots, with the total fitted curve as a solid line through the points. The edges were fitted to sums of a pseudo-Voigt step function (solid line) plus six pseudo-Voigt peaks. For the Cl K-edge the mixing parameters were held constant between the different fits, but the energies were allowed to vary. The energies of the two pre-edge features at 2821.2 and 2822.6 eV were found to be the same within experimental error for all spectra. Full details of the fits are given in the supplementary material.

al. for $(creatininium)_2CuCl_4$.[9] As the Cu $3d_{xy}$ orbital is closer in energy to $3d_{x^2-y^2}$ than to $3d_{xz}$,[41] changes in $1s \rightarrow 3d$ position and peak width would be more difficult to observe. Such (equatorial) $d\pi-d\pi$ bonding involving Cu $3d_{xy}$ orbitals is expected to be less important for $CuCl_2 \cdot 2H_2O$ due to the absence of accessible d orbitals on the oxygen ligands.

Chlorine K-Edge Spectra. The polarized single-crystal chlorine K-edge spectra of $CuCl_2 \cdot 2H_2O$, together with that of polycrystalline $CuCl_2 \cdot 2H_2O$, are shown in Figure 8. Three orientations are shown, with the **e**-vector oriented along [100], [010], and [001]. Unfortunately, a detailed study of the polarized chlorine K-edge XAS spectra was not possible because the crystals tended to lose water slowly to the helium atmosphere necessary for measurements at the low X-ray energies of the chlorine K-edge. Nevertheless, the three data sets in Figure 8 are highly informative. The spectra show significant anisotropy of all resolved spectral features, particularly in the sharp pre-edge feature at 2821.2 eV (Figure 8). This peak is most prominent when the **e**-vector is oriented along [001], the direction which is closest to the Cl−Cu vectors (see Figure 1), intermediate along [010], and smallest along [100], at 90° to the Cl−Cu bonds. When the **e**-vector is oriented along [100], some additional structure, a shoulder at 2822.6 eV, is also present. Peak deconvolutions of the spectra (Figure 8) suggest significant intensity for this second resonance along [010] and [001] as well, although in these cases, exact quantification is made more difficult by the proximity of the intense 2821.2 eV resonance. The curve-fitting analysis (see Figure 8) yields transition intensities for the 2721 eV resonance (peak areas, normalized to the edge jump) of 0.21, 0.93, and 1.35 along [100], [010], and [001], respectively, and 0.90 for the polycrystalline sample. Using eq 2, we can readily estimate the intensities along the molecular axis: $I_x = 2.12$, $I_y = 0.21$, and $I_z = 0.16$. The nonzero intensity in the y and z molecular directions may be accounted for by a combination of inaccuracies in the crystal alignment and the fact that the X-ray beam is less than 100% polarized. Our results clearly show that the 2821 eV resonance is intense along the molecular x axis, consistent with a dipole-allowed transition to a σ^* orbital associated with the Cu−Cl bond.

Pronounced pre-edge resonances of this type are not expected for chlorine in the formal Cl^- oxidation state, which would have full complement of 3p electrons, and it thus seems likely that covalency with the metal is involved. Sugiura *et al.*[42] have investigated the chlorine K-edges of $(NH_4)RhCl_6$ and K_3RuCl_6 and observed a pronounced pre-edge resonance at about 2821 eV very similar to the resonance which we observe in $CuCl_2 \cdot 2H_2O$. Nakai *et al.*[43] have observed similar pre-edge features in the fluorine K-edges of a number of first transition metal fluorides and have observed prominent pre-edge features for $3d^8$ NiF_2 and for $3d^9$ CuF_2 but not for $3d^{10}$ ZnF_2. More recently, Hedman *et al.*[44] also observed the presence of a 2821 eV resonance in the chlorine K-edge spectrum of two different $3d^9$ $CuCl_4^{2-}$ complexes but an absence of such a feature in a structurally analogous $3d^{10}$ $ZnCl_4^{2-}$ compound. Both Sugiura *et al.*[42] and Hedman *et al.*[44] assign the 2821 eV pre-edge peak as a transition to a σ^* antibonding orbital involving chlorine 3p and metal e_g d orbitals, and similar assignments of the fluorine K-edge pre-edge peaks were made by Nakai *et al.*[43] Interestingly, for K_3RuCl_6, Sugiura *et al.*[42] observe an even lower energy resonance (as a shoulder on the σ^* resonance) which they attribute to a $1s \rightarrow \pi^*$ resonance to an antibonding molecular orbital involving chlorine $3p\pi$ and metal t_{2g} orbitals. In support of the assignment of the 2821 eV peak, Hedman *et al.*[44] found that the intensity of the 2821 eV pre-edge resonance increased with the expected covalency of the Cl−Cu bonds for the two copper complexes investigated. More recently, Shadle *et al.*[45] investigated the chlorine K-edge spectra of a number of different cupric chloride complexes and examined the spectral trends with structural variations. Our observation of the polarization dependence of the 2821 eV resonance strongly supports the assignment of a $1s \rightarrow \sigma^*$ resonance to an antibonding orbital involving the Cu $3d_{x^2-y^2}$ orbitals,[44,45] which gains dipole-allowed intensity from covalent contribution of Cl 3p orbitals.[46] According to Hedman and co-workers,[44,45] the

(40) For this rather approximate calculation, we assume that the splittings between the two X-ray $1s \rightarrow 3d$ transitions is given by $\Delta E_{X-ray} = \Delta E_{orbital} + \Delta J_{d-d} - \Delta K_{d-d}$, where $\Delta E_{orbital}$ is the difference in orbital energies and ΔJ_{d-d} and ΔK_{d-d} are the differences in Coulomb and exchange energies, respectively. We assume that the transition we have assigned as $1s \rightarrow 3d_{x^2-y^2}$ corresponds to $[1s^2][3d^9] \rightarrow [1s^1][3d^{10}]$ and the $1s \rightarrow 3d_{xz}$ corresponds to $[1s^2][3d^8] \rightarrow [1s^1][3d^9]$. The Coulomb and exchange energies can be estimated using tabulated Racah parameters: (a) Lever, A. B. P. *Inorganic Electronic Spectroscopy*; Elsevier: Amsterdam, 1984. (b) Griffith, J. S. *The Theory of Transition Metal Ions*; Cambridge University Press: Cambridge, U.K., 1961.

(41) Hitchman, M. A. *J. Chem. Soc., Chem. Commun.* **1979**, 973−974.

(42) Sugiura, C.; Kitamura, M.; Muramatsu, S. *J. Chem. Phys.* **1986**, *84*, 4824−4827.

(43) Nakai, S.; Kawata, A.; Ohashi, M.; Kitamura, M.; Sugiura, C.; Mitsuishi, T. *Phys. Rev.* **1988**, *B37*, 10895−10897.

(44) Hedman, B.; Hodgson, K. O.; Solomon, E. I. *J. Am. Chem. Soc.* **1990**, *112*, 1643−1645.

(45) Shadle, S. E.; Hedman, B.; Hodgson, K. O.; Solomon, E. I. *Inorg. Chem.* **1994**, *33*, 4235−4244.

(46) The copper K-edge $1s \rightarrow 3d$ transition is not expected to gain dipole-allowed transition intensity from ligand covalency because of the very small overlap between the Cu 1s and Cl 3p orbitals.

orbital can be written as $\sigma^* = (1 - C^2)^{1/2}[\text{Cu } 3d_{x^2-y^2}] - C[\text{Cl } 3p]$, where C represents the amount of Cl 3p character in the antibonding molecular orbital. To a first approximation, the intensity of the transition is proportional to a generalized dipole-allowed pure 1s → Cl 3p transition weighted by the covalency C^2,[44,45] and the intensity of the pre-edge peak thus provides a convenient probe of ligand covalency.[47] In addition to studies of halide ligation,[42-45] previous studies have used such pre-edge peaks to probe ligand covalency using oxygen K-edges[48,49] and sulfur K-edges.[12] Hedman *et al.*[44] and Shadle *et al.*[45] have used this relation to estimate covalencies for a number of different Cu−Cl compounds using an EPR-derived covalency for $(\text{creatininium})_2CuCl_4$ as a reference. Using their relationship [$C \approx 0.128I$, where I is the 2821 eV peak area normalized to the edge jump], we estimate a covalency per Cl for $CuCl_2 \cdot 2H_2O$ in the range 0.11−0.12,[50] which is significantly larger than those for $CuCl_4^{2-}$ compounds[44,45] but consistent with the presence of less strongly donating oxygen ligands, which should cause an increase in the charge donation by the chlorides.[45]

Conclusions

We have presented a detailed experimental study of the polarized copper K-edge near-edge spectrum of $CuCl_2 \cdot 2H_2O$ and have shown the essentially pure quadrupole nature of the 1s → 3d transition in this compound. The maximum amplitude of the 1s → 3d transition is ≈4% of the edge jump, which is in good agreement with the theoretical values calculated by Bair and Goddard[6] and by Yokoyama *et al.*[10] The additional 1s → 3d intensity which we observe on rotating the crystal as detailed in Figure 7B can be attributed to copper d vacancies in the $3d_{xz}$ orbital, caused by dπ−dπ back-bonding with the chlorine ligands. The orientation dependence of the Cu K-edge dipole-allowed transitions is in excellent agreement with the theoretical calculations of Yokoyama *et al.*,[10] and in particular the previously controversial 1s → $4p_z$ + ligand-to-metal charge transfer shakedown transition now seems firmly established. Our chlorine K-edge experiments confirm and extend the assignments of earlier workers[42-46] that the pronounced pre-edge peak is due to a 1s → σ* transition to an antibonding orbtial involving both Cl 3p and Cu $3d_{x^2-y^2}$ orbitals.

Acknowledgment. This work was done partially at SSRL, which is funded by the Department of Energy, Office of Basic Energy Sciences. The Biotechnology Program is supported by the NIH, Biomedical Research Technology Program, Division of Research Resources. Further support is provided by the Department of Energy, Office of Health and Environmental Research. The NSLS is funded by the Division of Materials Sciences, U.S. Department of Energy, under Contract DE-AC02-76CH-0016. We are indebted to Roger C. Prince and Michael Sansone of Exxon Research and Engineering Co. for their assistance with the collection of the chlorine K-edge data and to Paul Stevens also of Exxon Research and Engineering Co. for helpful discussions. A large part of this paper was written while the authors were guests at the Department of Inorganic Chemistry, University of Sydney, Australia. We thank Professor Hans Freeman and his colleagues at the Department of Inorganic Chemistry for their hospitality during our stay and the Foundation for Inorganic Chemistry at the University of Sydney for financial support which made our visit possible.

Supplementary Material Available: Full results of curve-fitting Cu K-edge spectra of single-crystal and powder $CuCl_2 \cdot 2H_2O$ (Table S1 and Figure S1) and full results of curve-fitting Cl K-edge spectra of single-crystal and powder $CuCl_2 \cdot 2H_2O$ (Table S2) (10 pages). Ordering information is given on any current masthead page.

IC941299N

(47) A similar, but inverted, correlation with covalency has been observed for the intensity of the dipole-allowed 2p → 3d transitions in copper L_{III}- and L_{II}-edges (George, S. J.; Lowery, M. D.; Solomon, E. I.; Cramer, S. P. *J. Am. Chem. Soc.* **1993**, *115*, 2968−2969).

(48) de Groot, F. M. F.; Grioni, M.; Fuggle, J. C.; Ghijsen, J.; Sawatzky, G. A.; Petersen, H. *Phys. Rev.* **1989**, *B40*, 5715−5723.

(49) Pedio, M.; Fuggle, J. C.; Somers, J; Umbach, E.; Haase, J.; Lindner, Th.; Höfer, U.; Grioni, M.; de Groot, F. M. F.; Hillert, B.; Becker, L.; Robinson, A. *Phys. Rev.* **1989**, *B40*, 7924−7927.

(50) We estimate this range from the fits to the single-crystal data [$I = (I_x + I_y + I_z)/3$, $C = 0.11$] and the fit to the polycrystalline sample [$C = 0.12$].